Pitfalls and considerations in determining the potency and mutant selectivity of covalent epidermal growth factor receptor inhibitors

Kristopher W. Hoyt,[1a] Daniel A. Urul,[1b] Blessing C. Ogboo,[a] Florian Wittlinger,[c] Stefan A. Laufer,[c,d,e] Erik M. Schaefer,[2b] Earl W. May,[2b] and David E. Heppner[2a,f]

a- Department of Chemistry, University at Buffalo, The State University of New York, Buffalo, NY, 14260, USA
b- AssayQuant Technologies, Inc., Marlboro, MA, 01752, USA
c- Department of Pharmaceutical and Medicinal Chemistry, Institute of Pharmaceutical Sciences. Eberhard Karls Universität Tübingen, Auf der Morgenstelle 8, 72076 Tübingen, Germany
d- Cluster of Excellence iFIT (EXC 2180) "Image-Guided and Functionally Instructed Tumor Therapies" Eberhard Karls Universität Tübingen, 72076 Tübingen, Germany
e- Tübingen Center for Academic Drug Discovery & Development (TüCAD2), 72076 Tübingen, Germany
f- Department of Pharmacology and Therapeutics, Roswell Park Comprehensive Cancer Center, Buffalo, NY, 14203, USA

[1]These authors contributed equally
[2]Co-corresponding davidhep@buffalo.edu, earl.may@assayquant.com, erik.schaefer@assayquant.com

Abstract

Pursuing enzyme inhibitors with molecules that form covalent bonds with the desired target is an attractive focus in drug development that is increasing in prevalence. However, challenges arise when carrying out assessments of their time-dependent inhibitory properties as well as making correlations with values reported in the literature. Given the prominent focus on the Epidermal Growth Factor Receptor (EGFR) tyrosine kinase in oncology, and the diverse structures and binding modes of covalent EGFR inhibitors, this perspective seeks to explore various broadly relevant factors that arise in the measurement of kinetic parameters within this class of drugs. A review of several studies indicates that variable literature potency values require investigators to include appropriate reference molecules and consistent substrate conditions for experimental consistency and proper benchmarks. The impact on covalent inhibitor potency with respect to common buffer conditions and compound liquid handling is surveyed highlighting the importance of multiple experimental variables when conducting these assays. Additionally, when assessing the potency for inhibitor selectivity in targeting EGFR mutants over wild-type (WT), it is ideal to consider ratios of true potency due to the variable ATP substrate binding affinities. The overview presented here, although most directly applicable to the tyrosine kinase inhibitor field, serves inhibitor assessments broadly by providing guided insights into conducting biochemical assays for designing and validating next-generation covalent inhibitors.

Introduction

The rational design of inhibitor molecules that form covalent bonds with their targets is routinely pursued in drug discovery.[1-5] Despite initial hesitations, covalent inhibitors are well established to possess highly desirable drug characteristics including potency, selectivity, and residence times, which has led the way to approximately 50 FDA-approved drugs.[6] The clinical efficacy of covalent inhibitors often

comes from their superior target residence times enabled through their deliberate inability to dissociate from the target upon covalent bond formation.[7] Recent clinically-deployed examples include molecules targeting the epidermal growth factor receptor (EGFR),[8] Bruton's tyrosine kinase (BTK),[9, 10] K-Ras,[11-14] and the main protease of the SARS-CoV-2 coronavirus.[15] These complexes have been designed to take advantage of specific reversible-binding properties that subsequently direct covalent bond formation at nucleophilic cysteine residues. Importantly, the choice of warhead chemistry determines whether the covalent drug is reversible or irreversible by design.[4, 5] Another element is that some irreversible warheads are themselves less stable, which emphasizes the importance of empirical measurements to confirm the nature of the association over time. While a persistently growing repertoire of targetable amino acid side chains by diverse covalent warheads enhance a drug developer's arsenal,[16, 17] rational design of new covalent inhibitors will rely on tailor-made screening techniques with added complexity to properly distinguish the performance of emerging inhibitor molecules.

EGFR inhibitors

EGFR is the prototypical member of the ErbB-family of receptor tyrosine kinases (RTKs).[18, 19] Aside from their implications across ordinary (healthy) biology, EGFR is a frequently mutated oncogene where alterations in the protein structure of the EGFR protein leads to aberrant signaling in cancer.[20, 21] Tyrosine kinase inhibitors (TKIs) are often effective therapies for non-small cell lung cancer (NSCLC) patients where their tumors are established to harbor activating mutations within the EGFR kinase domain.[22, 23] First-generation anilinoquinazoline TKIs erlotinib and gefitinib were previously approved for mutant EGFR NSCLC, but the third-generation inhibitor AZD9291 (osimertinib) has more recently been shown to be more effective as a front-line drug.[24] Originally, osimertinib was designed based on tool compounds (e.g., WZ4002)[25] that exhibited selectivity toward the T790M gatekeeper mutation, which is the primary route to drug resistance for first-generation TKIs.[24] Osimertinib is an irreversible inhibitor that, just like WZ4002, forms a covalent bond to the non-catalytic cysteine residue C797 near the ATP-binding site. Patients acquire resistance to osimertinib through several routes, most notably when the EGFR kinase domain mutates the cysteine to a serine (C797S), which is incompatible with the molecule's covalent bond forming Michael acceptor group.[26, 27] While efforts are currently underway to address C797S and other modes of osimertinib-induced drug resistance,[28, 29] drug development has continued to optimize third-generation compounds, such as the recently emerged YH25448 (lazertinib)[30, 31] to improve various pharmacological properties (e.g., dose-limiting toxicity). Given the continued activity around optimizing irreversible EGFR TKIs it is important to properly understand the structural differences in established covalent EGFR TKIs and the assays used to accurately judge their potency and selectivity for EGFR variants including WT and the activating mutations responsible for drug resistance.

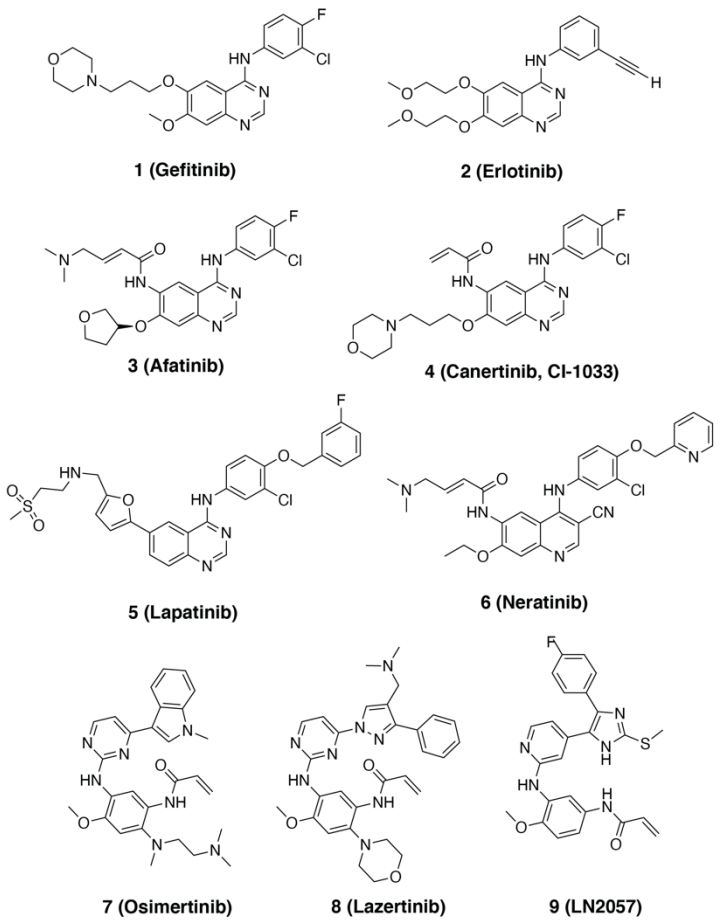

Scheme 1. Chemical structures of selected EGFR inhibitors.

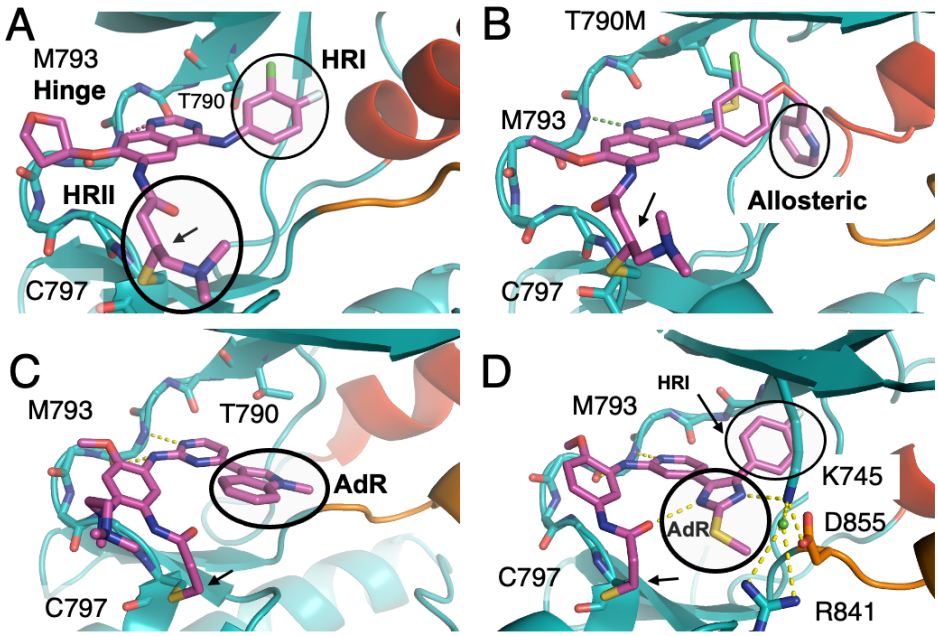

Figure 1. Binding modes of representative irreversible C797-targeting EGFR inhibitors. X-ray cocrystal structures **highlighting the binding modes** of (A) afatinib with WT EGFR (PDB ID 4G5J), (B) neratinib with T790M EGFR (PDB ID 2JIV), (C) osimertinib with WT EGFR (PDB ID 6JXT), (D)

LN2057 with WT EGFR (PDB ID 6VHN). Pocket labels denote the functional group of the visualized inhibitor that occupies the given pocket. Black arrows near C797 indicate the carbon atom of the inhibitor that is covalently bonded to the C797 sulfur. Regions labeled consistent with nomenclature from reference [32].

The earliest iterations of covalent (second-generation) inhibitors targeting EGFR were based on the anilinoquinazoline-scaffolds similar to erlotinib and gefitinib (Scheme 1). Incorporation of a Michael acceptor warhead to target the aforementioned C797 residue near the ATP binding site, initially done by chemists from Parke Davis (a subsidiary of Pfizer since 2000), produced a superiorly potent irreversible inhibitor and eventual FDA-approval of afatinib[33, 34] and dacomitinib[35] for EGFR-mutant lung cancer. The closely-related CI-1033 (canertinib) is a well-studied inhibitor originally being investigated by Pfizer. Despite development being discontinued, it is still important for points made later on in this perspective.[36] Structurally, afatinib binds the EGFR kinase catalytic cleft by anchoring groups within three regions, specifically the quinazoline core is anchored to the hinge region at M793 through an H-bond, a substituted phenyl ring within the hydrophobic region I (HRI), and the covalent warhead that forms the covalent bond with C797 in the hydrophobic region II (HRII) (Figure 1A). (It is important to note that many of these regions within the kinase inhibitor binding site are known by different names, and we have followed the nomenclature set out by Lui and Gray, 2006[32]). Neratinib is a unique irreversible second-generation TKI in that it stabilizes the inactive (αC-helix out) form of the kinase by binding a pyridine group anchored from HRII into the allosteric pocket (Figure 1B), a feature not seen in other second-generation EGFR TKIs. Neratinib shares this unique structural motif (pyridine versus fluorobenzyl) and property in common with the reversible inhibitor lapatinib and it is often classified as a type 1.5 TKI due to the requirement for this inhibitor to reinforce the αC-helix out inactive conformation rendering the mechanism both ATP-competitive and allosteric.[37] It is noteworthy to mention that this phenyl ring in the allosteric pocket corresponds to recently reported mutant-selective allosteric inhibitors[38-45] and ATP-allosteric chimeric molecules.[46-48]

Third-generation inhibitors possessing an alternative hinge binding anilinopyrimidine scaffold were breakthrough molecules possessing T790M-selectivity[25] and led the way for FDA approval of AZD9291 (osimertinib).[24, 49] The anilinopyrimidine scaffold exemplifies the utility of irreversible inhibitors as it enables weak but selective binding to T790M mutant harboring kinases and is made uniquely potent by the formation of the covalent bond to C797.[25, 50] The pyrimidine core binds to the hinge through two H-bonds and, different to quinazoline inhibitors, harbors an *N*-methylindole extending away from the adenosine-binding region (AdR) and not into HRII (Figure 1C). The structural origin of the T790M-selectivity has been attributed to productive intermolecular van der Waals interactions with the mutant methionine side chain recently characterized by the comparison of soaked and cocrystallized EGFR kinase domain structures coupled to MD simulations.[51] A newer third-generation TKI developed by Yuhan and Janssen (YH25448, lazertinib) has shown marked improvements over osimertinib in terms of diminished dose-limiting toxicity and HER2 off-target inhibition, while utilizing similar van der Waals interactions with T790M, in addition to novel H-bonding, to afford effective and preferential EGFR mutant targeting.[30, 31, 52, 53] Distinctly, several lead compounds have been developed and exhibit inhibition of C797S-containing kinase domains from various EGFR mutant variants. Important examples of such are trisubstituted imidazole molecules, which were the earliest instances of C797S-targeting inhibitors and lead to a variety of irreversible analogues being produced (LN2057 Scheme 1, Figure 1D). These compounds, which bind an imidazole in the AdR as well as a 4-fluorophenyl to HRII, are made potent against C797S EGFR through extra H-bonds to conserved catalytic residues. Molecules of this type are not mutant selective, and exhibit high WT potency, but share structural elements with C797S mutant-selective inhibitors.[28] The molecules featured in Scheme 1 and Figure 1 are well-studied and are examples

of the diverse binding modes for covalent EGFR TKIs, which are informative for understanding the methods utilized to determine and interpret their potency and mutant-selectivity.[21, 28]

Kinetics of Covalent Inhibitors

All irreversible EGFR TKIs bind and inactivate EGFR tyrosine kinase activity in a two-step process. The first process is a rapid equilibrium that forms the non-covalent E·I complex, described by the dissociation constant, K_i (Figure 2, Eq 3), followed by an irreversible covalent adduct formation (E-I), defined by the rate constant, k_{inact} (Figure 2). For a particular TKI, one can assess the potency through the composite second-order inhibitor potency (k_{inact}/K_I, Eq 1) that reflects the time-dependence of inhibition from free enzyme (E) to fully inactivated enzyme-inhibitor complex (E-I). The expression for k_{inact}/K_I is dependent on all of the rate constants that govern target inhibition (Eq 1) and is the most important term in assessing covalent inhibitor structure activity relationships (SARs) or more appropriately structure kinetic relationships (SKRs). Separately, the inactivation constant, K_I, is the inhibitor concentration required to inactivate the enzyme at $½k_{inact}$.[54] Similar to K_M for enzyme substrates, K_I can be seen as a composite of the rate constants describing the fate of the noncovalent E·I complex (Eq 2). Determination of the irreversible inhibitor potency can be done by the obtaining observed rate constant (k_{obs}) as a function the inhibitor concentration [I]. This plot for irreversible inhibitors yields a hyperbola where the upper asymptote is k_{inact}, the [I] at half maximal k_{obs} is K_I, and the slope of the initial linear approximation of the hyperbola is k_{inact}/K_I. This traditional analysis method can prove productive, but only accounts for variations in k_{obs}. A far better method is available which incorporates all the information in the primary data to yield not only k_{obs}, but also the initial reaction rate, and these values are determined with higher confidence. Here, the formation of phosphorylated product (P) can be monitored through progress curves as generated from a 24-point 1.5-fold dilution series on a single plot (Figure 3, See supporting information for method details). A global fit of all the data yields a much stronger fit, and statistical tests can be done to determine if a one-step fit (yielding k_{inact}/K_I) or two-step fit (yielding k_{inact} and K_I separately) is most appropriate. It is also important to emphasize a recurring point of confusion in this field regarding K_i versus K_I. There are cases where investigators correctly give values for k_{inact}/K_i (e.g., [53]) and others where "k_{inact}/K_i" is listed but the method actually reports k_{inact}/K_I. There are instances where K_i approximates K_I (when $k_{-1} >> k_{inact}$, Eq 2), but they are rarely interchangeable.[51] In any event, attention to the details of these parameters is of utmost importance.

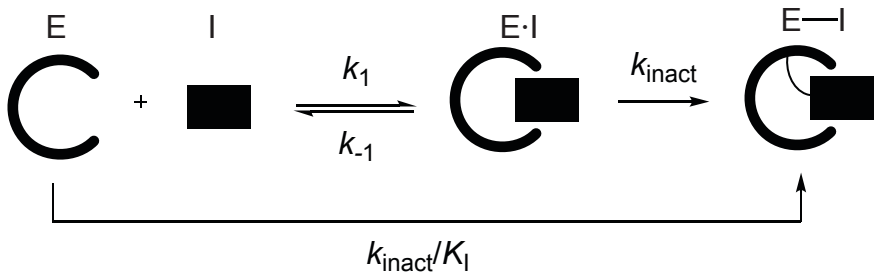

Figure 2. The two-state inactivation of an enzyme target by an irreversible inhibitor.

$k_{inact}/K_I = \frac{k_1 k_{inact}}{k_{-1} + k_{inact}}$	**(Equation 1)**
$K_I = \frac{[E][I]}{[E \cdot I]} = K_i + \frac{k_{inact}}{k_1} = \frac{k_{-1} + k_{inact}}{k_1}$	**(Equation 2)**
$K_i = \frac{k_{-1}}{k_1}$	**(Equation 3)**
$P = \frac{V_i}{k_{obs}} (1 - e^{- k_{obs} t})$	**(Equation 4)**

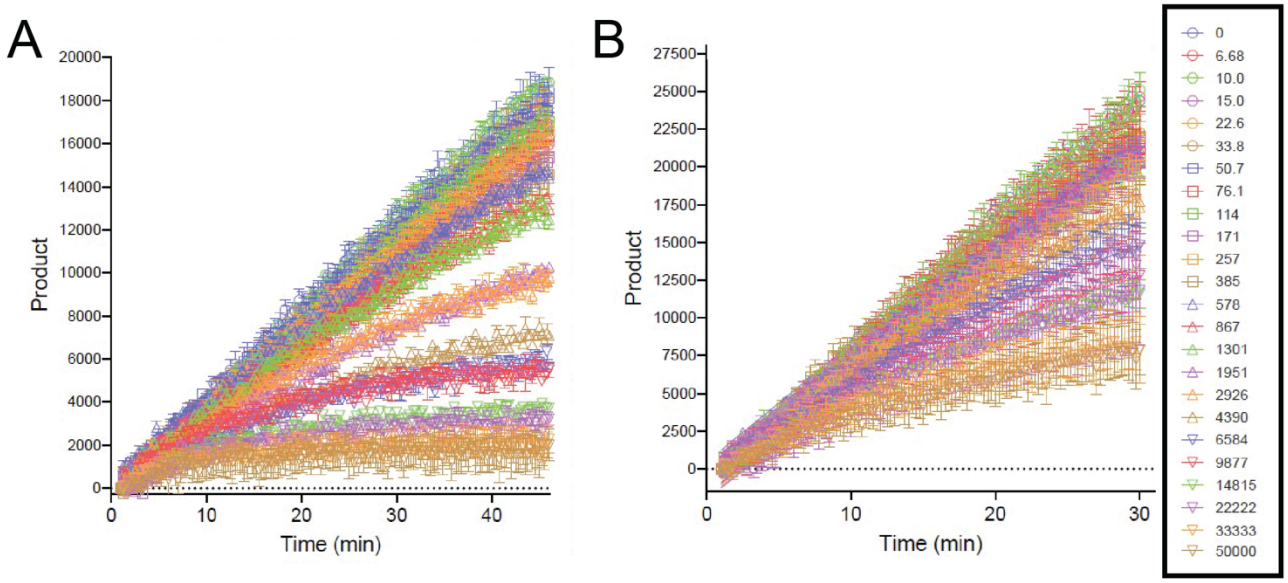

Figure 3. Illustrative examples of time-dependent process curves. Measurements of product formation with a covalent inhibitor dosed against EGFR A) WT and B) L858R/T790M kinase domains. Data generated from a 24-point 1.5-fold dilution series.

Methodological diversity in measuring time-dependent kinetics for irreversible EGFR TKIs.

The optimization of any drug compound relies on various assays to assess SARs to deliver several lead molecules. Unlike reversible-binding inhibitors that can be readily compared on the basis of IC_{50} values, irreversible inhibitors require more sophisticated dynamic experiments to properly assess potency (k_{inact}/K_I) and ideally the constituent kinetic parameters k_{inact} and K_I. Reliance solely on IC_{50} values to guide SARs for irreversible inhibitors can be misleading, and proper evaluation of kinetic parameters are needed for the more proper SKR. In this section, we will review the methods that have been used previously to assess the time-dependent behavior of irreversible EGFR TKIs with the ultimate goal of providing context for variables that may impact experimental outcomes.

The general experimental set up for assessing irreversible inhibitor potency involves a dynamic readout of enzyme activity ideally performed in a 96- or 384-well microplate to capture a wide range of inhibitor concentrations simultaneously at comparable conditions. For assessing the activity of irreversible EGFR TKIs, investigators have utilized several methods including 1) progress curve analysis (PCA), 2) incubation time-dependent potency $IC_{50}(t)$, and 3) stopped-flow (SF) double mixing. PCA requires an assay method that monitors the dynamics of EGFR substrate phosphorylation, and the majority of studies[50, 53, 55] have utilized sulfonamido-oxine (Sox)-peptide reagents that enable assays to measure substrate phosphorylation with fluorescence in a continuous, direct and quantitative format.[56-58] In our experiments, for example,[53] we find that such studies should be conducted to maximize the number of time points collected where possible to enable accurate global fitting. The continuous nature of the Sox-based PhosphoSens platform from AssayQuant Technologies, Inc. provides flexibility to collect the most appropriate regions of the progress curve, and this is done for every condition and in every well of the 96- 384- or 1536-well microplate. Importantly Sox was designed to be small and minimally hydrophobic (very similar to tryptophan) to avoid artifacts seen with other larger fluorophores commonly used in kinase activity series. Another approach has been developed that allows for the determination of time-dependent inhibition values by comparing IC_{50} values at different times after initial enzyme incubation with inhibitor.[59, 60] Typically, IC_{50} values alone are inappropriate to assess covalent inhibitor potency,[54] whereas this method utilizes an implicit time-dependent expression for obtaining k_{inact} and K_I that is amenable to alternative end-point assays, such as HTRF.[61] There have been reports of liabilities in the $IC_{50}(t)$ method that pertain to drug preincubation with enzyme (common for IC_{50} value determination) that can overestimate k_{inact} and underestimate k_{inact}/K_I.[62] Alternatively, double mixing experiments with an SF spectrofluorometer have been utilized to determine k_{inact} values directly where an initial pre-incubation of EGFR kinase domain proteins with osimertinib are subsequently mixed with substrates allowing for measurement of displaced non-covalently bound osimertinib.[50] These methods represent the diverse approaches available for irreversible inhibitor potency determination, although as is the case for many biochemical assays, it can be challenging to know how best to compare results between such studies, especially if the experimental methods are incompletely described as is commonly observed.

Experimental considerations

Any drug characterization assay, if biochemical or cell-based, requires decisions that may influence the method leading to erroneous or inconsistent results. We sought to better understand a variety of experimental conditions in our own PCA SOX-based EGFR assays originating from a recent study on irreversible EGFR TKIs.[53] The Sox-based PhosphoSens platform can use low or high ATP concentrations and we typically perform assays using 1 mM ATP, which is physiological. Alternatively, assays can be run at with an ATP concentration near the enzyme K_M value. With the EGFR, we use AQT0734 as the

optimized Sox-sensor peptide substrate, which allows low nM detection of WT and mutant kinase variants. This substrate is derived from a physiologically-relevant protein substrate. Generally, we prepare a low volume (6 µL) of ATP, Sox substrate, and the inhibitor, which is mixed together with a larger volume (14 µL) of a master mix containing buffer and recombinant EGFR protein (see protocols in supporting information). Previously, we had prepared this initial low volume solution with 10-times concentration solution of ATP substrate, SOX peptide substrate, and inhibitor where the inhibitor was added as a solution of 10% DMSO in water such that after mixture with the rest of the assay components, it would be normalized to 1% DMSO, which generated successful functional assessment to determine the potency relationships between lazertinib, osimertinib, and LN2057 (10x PCA, Table 1).[53] An alternative protocol eventually became necessary in subsequent studies due to compound solubility issues observed with certain compounds (unrelated, unpublished work) where 100-times solutions (in 100% DMSO) of inhibitor were added to ATP and SOX peptide substrate prior to reaction initiation with minor adjustments in reaction mixture volumes to ensure proper final concentrations of components in 1% DMSO. Unexpectedly, when applied to the current study in this perspective, this inhibitor preparation method led to enhancement in k_{inact}/K_I values for all three compounds with a range of values: 2.5- to 7.9-fold for the WT EGFR and 3.1- to 10.9-fold for the L858R/T790M mutant, with the magnitude of this shift being osimertinib > LN2057 > lazertinib (100x PCA Table 1). Interestingly, the differences appear to be mainly due to an apparent reduction in K_I while k_{inact} remains largely unaffected.

While the exact origins of this enhancement in inactivation constants are undetermined, our observations suggest this increase in k_{inact}/K_I potency may result when taking the unique solubility properties of the inhibitors tested. The fact that this increase in potency happens with all 3 compounds and that the rank order of the change in potency is similar with both the WT and mutant enzyme, presumably reflects a pharmacological property of the compounds where the use of 100% DMSO improves solubility given these assay conditions. The literature is rich with publications seeking to identify a collection of physicochemical or thermodynamic properties of compounds that predict compound behavior, including solubility, in an aqueous environment.[63-65] The topological polar surface area (TPSA) is a commonly-used parameter that provides important insights given certain ligand-receptor interactions and relevant biological conformations with proteins. including H-bonding. TPSA is defined as the surface sum over all polar atoms or molecules, primarily oxygen and nitrogen, also including their attached hydrogen atoms.[63] TPSA is often used to predict cellular absorption for which has been reported the optimum TPSA range as 60–140 $Å^2$.[65] Intriguingly, the TPSA values for the above 3 compounds are osimertinib (87.6 $Å^2$) > LN2057 (91.9 $Å^2$) > lazertinib (110 $Å^2$), which is the same rank order for the increase in k_{inact}/K_I observed with our 100x PCA method (100% DMSO). Additional work will be required to test this hypothesis, which highlights a key need to understand how different physicochemical properties affect functional potency under different compound treatment and assay conditions.

Aside from liquid handling, several other important variables need to be defined regarding common assay reagents, assay conditions, and the source of recombinant enzyme. The majority of drug development laboratories do not readily make their own recombinant kinase domains, and routinely acquire them from commercial suppliers. Important differences can include the construct size, tag, tag location, host expression system, and purification methods. We find that readily available enzymes (Signal Chem and Carna) are consistently inhibited by osimertinib with the PCA 100x method (Table 2). The choice of peptide substrate is also important. In our studies we have used the AQT0734 Sox-peptide reagent, which is a physiologically-relevant substrate. In contrast, many studies use synthetic peptides (e.g., polyGlu-Tyr) or sequences that have been extensively modified with multiple terminal lysine or arginine residues to facilitate binding to phosphocellulose (P81) paper, which we have seen can dramatically change the interaction with the target kinase. Additionally, kinases often require the

presence of excess reductant to prevent inactivating oxidation and deterioration of the enzyme proteins. A common reductant included in kinase domain buffers is dithiothreitol (DTT, Cleland's Reagent), which contains two thiol groups that have the ability to react with the electrophilic warheads in irreversible kinase TKIs, potentially rendering them less active when measuring inhibitor potency. Another common reagent included in protein kinase activity assays is bovine serum albumin (BSA) protein, which contains a reactive cysteine thiol and may also react with inhibitor electrophilic groups. Kinetic parameters determined in the presence and absence of DTT and BSA with osimertinib show no significant differences compared to assays performed in the presence of reductant tris(2-carboxyethyl)phosphine (TCEP) and no BSA (Table 2). These comparable kinetic values indicate that the inclusion of BSA and DTT reagents are not contributing to the observed differences in potency in these biochemical assays. Although no significant perturbations are observed here rigorous assessment of any given irreversible inhibitor for effects of such buffer additives is still warranted. In any case, these comparisons clearly indicate that for osimertinib, inhibition of EGFR is most impacted by alterations in inhibitor liquid handling.

Comparing irreversible inhibitor potencies across EGFR TKIs studies

Osimertinib is the most frequently measured irreversible EGFR inhibitor and most informative regarding the consistency between studies. Table 1 shows a set of values determined from all of the methods mentioned earlier against WT, L858R and L858R/T790M EGFR variants. It is generally seen that potency values $(k_{inact}/K_I)^{app}$ for osimertinib vary significantly, while the inactivation rate k_{inact} is generally consistent across studies in all three enzymes (Table 1). A study by scientists at AstraZeneca employed several enzymatic kinetics techniques (PCA and SF) to better characterize the potency of osimertinib, and it is a thorough kinetic study of EGFR TKIs.[50] In their PCA assays, the investigators were unable to obtain two-step fits necessary to determine individual k_{inact} and K_I values, but report true and apparent k_{inact}/K_I due to limited reversible binding (Table 1). Another series of studies have reported osimertinib activity utilizing the $IC_{50}(t)$ method allowing for the determination of k_{inact}/K_I and the individual components (Table 1).[59, 66, 67] Overall, and including our earlier values,[53] the osimertinib apparent potencies (k_{inact}/K_I) are quite different and this presumably reflects the diversity in compound treatment and assay conditions used for these determinations, the rank order of potencies is the same (L858R > L858R/T790M > WT), and this is consistent with the mutant-selectivity of this drug. The $IC_{50}(t)$ method deviates from this trend slightly showing osimertinib to be slightly more potent against L858R/T790M compared to L858R.[59, 66, 67] k_{inact} values from our experiments are mostly comparable with the rates obtained from SF double mixing, all being faster than PCA and $IC_{50}(t)$. Lazertinib potency also matches the trend in k_{inact}/K_I values (L858R > L858R/T790M > WT), is consistent with its T790M selectivity, and the non-selective LN2057 is superiorly potent against L858R, but less so for L858R/T790M. This global comparison (Table 1) shows that k_{inact}/K_I values are relatively difficult to compare, and the differences could be due to a variety of experimental factors, but general trends from mutant and WT EGFR appear more comparable.

Second-generation EGFR TKIs

Given the trend in apparent potency values across the EGFR variants for third-generation inhibitors, it is informative to consider how these trends compare to second-generation TKIs. Since most of the attention in this field has focused on osimertinib and other third-generation TKIs, we independently obtained kinetic values for second-generation inhibitors afatinib, canertinib (CI-1033), and neratinib to compare with our earlier experiments (PCA 100x, Table 3). It is observed that potency against L858R is higher for these compounds comparted to WT, similarly reflecting stronger reversible inhibitor binding, consistent with the lower K_M for ATP.[68] In contrast to osimertinib and lazertinib, these three compounds

are significantly less potent against L858R/T790M, showing lower k_{inact}/K_I compared to WT. This is consistent with the notion that acquisition of the T790M mutation renders these inhibitors ineffective and their clinical application leads to drug resistance. In the case of afatinib, the trend in potency values is consistent with earlier work.[50] The principal source of the different potencies observed are all related to changes in K_I, with k_{inact} remaining fairly consistent, indicating that differences in selectivity and potency are enabled by alterations in reversible binding properties.

Assessing Covalent Inhibitor Mutant Selectivity

An important distinguishing feature of covalent EGFR TKIs is their ability to inhibit specific activating EGFR mutants while simultaneously having limited activity against the WT protein. In this way, the biochemical behavior of EGFR TKI potency is of vital significance and assessing mutant selectivity must be a consideration at all points in the development process. It is well recognized that reversible-binding first-generation TKIs, such as erlotinib and gefitinib (Scheme 1), are stronger binders with EGFR(LR) due to the significantly weaker ATP-binding affinity compared to WT.[68, 69] Acquired resistance to these inhibitors results in an additional T790M point mutation that renders first-generation TKIs ineffective by enhancing the ATP affinity to approximate the same affinity for WT.[70] As such, the variability in K_M of the ATP substrate in an enzyme that is the target if a covalent ATP-competitive inhibitor is a key determining factor in assessing if a given compound is likely to be clinically effective (i.e., exhibit an ideal therapeutic window).[20]

As a practical matter, it is worth considering variabilities often observed in kinetic parameters that are routinely used to assess inhibitor potency and selectivity. For reversible inhibitors, enzyme inhibition experiments that enable the determination of IC_{50} values are informative and simpler than determining inhibition constants (K_i). Despite their convenience, IC_{50} values are "apparent" in that they vary with respect to ATP substrate concentrations whereas the dissociation constant is invariant (i.e., absolute or "true"). The relationship between these two parameters for competitive inhibitors is given by the Cheng-Prusoff equation (Eq. 5).[71, 72] For covalent inhibitors, k_{inact}/K_I measured in any given experiment is similar to the IC_{50} in that they both vary with respect to ATP concentration, and for the sake of this perspective, that is where their comparability ends. Calculation of a "true" k_{inact}/K_I is possible through an equation that resembles the Cheng-Prusoff equation for ATP competitive reversible inhibitors (Eq. 6).[50] In this respect, the variabilities in a specific kinase K_M and the ATP concentration in a specific experiment can be eliminated for more direct comparison of the properties of covalent TKIs.

$IC_{50} = K_i (1 + [ATP]/K_M)$	**(Equation 5)**
$(k_{inact}/K_I)^{true} = (k_{inact}/K_I)^{app} (1 + [ATP]/K_M)$	**(Equation 6)**

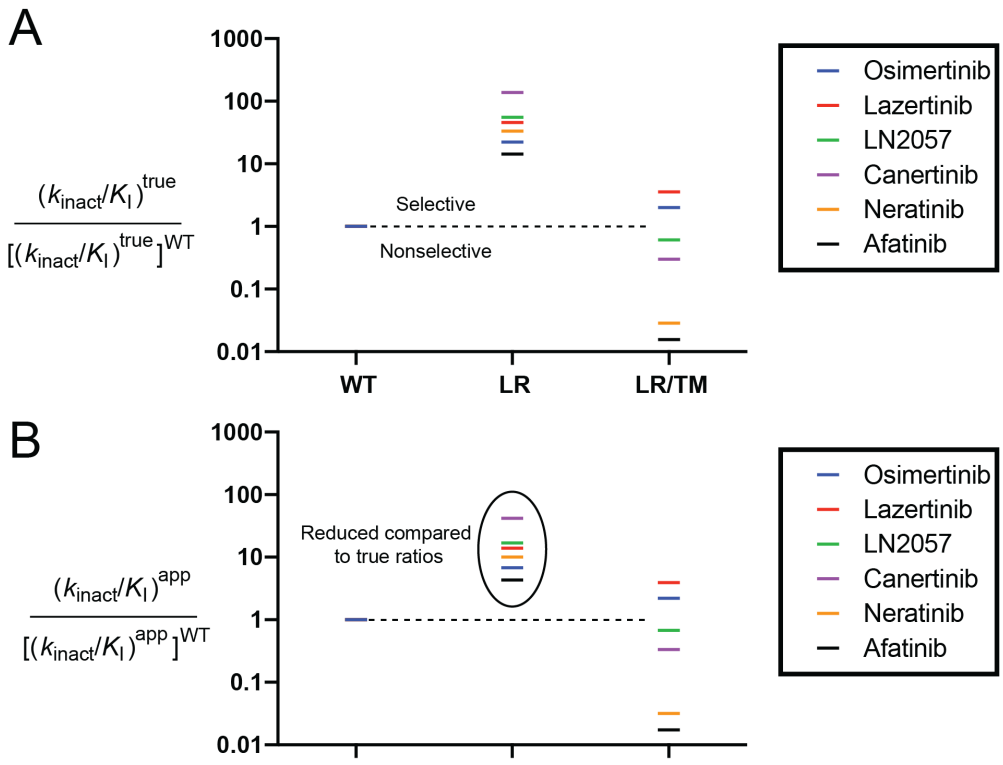

Figure 4. Defining reversible TKI mutant selectivity. Graphical representation of apparent potency A) $(k_{inact}/K_I)^{true}$ B) $(k_{inact}/K_I)^{app}$ ratios for WT, L858R (LR) and L858R/T790M (LR/TM) normalized to EGFR WT. Mutant selectivity for L858R/T790M can be assessed based on the $(k_{inact}/K_I)^{app}$ ratio being above or below the WT values. True (k_{inact}/K_I) values are obtained on the basis of K_M values from Zhai et al. [50]

Given the above consideration, a reasonable question in any drug development effort would be: "Is the $(k_{inact}/K_I)^{true}$ or $(k_{inact}/K_I)^{app}$ value most ideal for assessing mutant selectivity of covalent inhibitors?". Adherence to kinetic rigor requires selectivity to be made on the basis of invariant true potency values.[54] On the other hand, an argument could be made for assessing selectivity on the basis of apparent rates, with assays performed at identical and sufficiently high ATP substrate concentrations, that would reflect the inhibition of an enzyme given the variabilities in K_M for ATP. One may suggest that apparent potency values would more accurately reflect biological conditions where ATP concentrations in cells are typically much higher (i.e., millimolar values) than target K_M values for ATP. To better understand the mutant selectivity of a subset of irreversible TKIs, a plot can be generated showing trends in mutant potency normalized by WT potency (Figure 4). In this case, we have conducted experiments based on the PCA 100x protocol (Supporting Information) at 1 mM ATP concentration for six distinct covalent EGFR inhibitors. Normalizing the true (Figure 4A) and apparent (Figure 4B) to the corresponding WT values returns the exact same behavior for all six of these molecules in inhibition assays for WT, LR, and LR/TM EGFR variants. All six inhibitors show selectivity for LR, as consistent with the lower ATP binding affinity for this mutant, and then potency values fall for LR/TM. Osimertinib and lazertinib are found to inhibit LR/TM with higher potency than WT, as consistent with their established TM selectivity. The remaining four inhibitors are well-accepted to be ineffective against TM and their potency falls below the corresponding WT value. $(k_{inact}/K_I)^{true}$ LR ratios are generally higher than those for $(k_{inact}/K_I)^{app}$ on account of the higher K_M values for ATP. Provided the mutant K_M values for ATP are the same or higher than WT, the invariant $(k_{inact}/K_I)^{true}$ potencies will exhibit a greater fold

difference compared to the corresponding apparent values. It seems reasonable given what is known about EGFR kinase K_M values for ATP to assess mutant selectivity by ratios of $(k_{inact}/K_I)^{true}$ values. When evaluating distinct covalent inhibitor development with other targets, one should carefully consider the impact of K_M for ATP substrate variance for confidence in assessing covalent inhibitor selectivity.

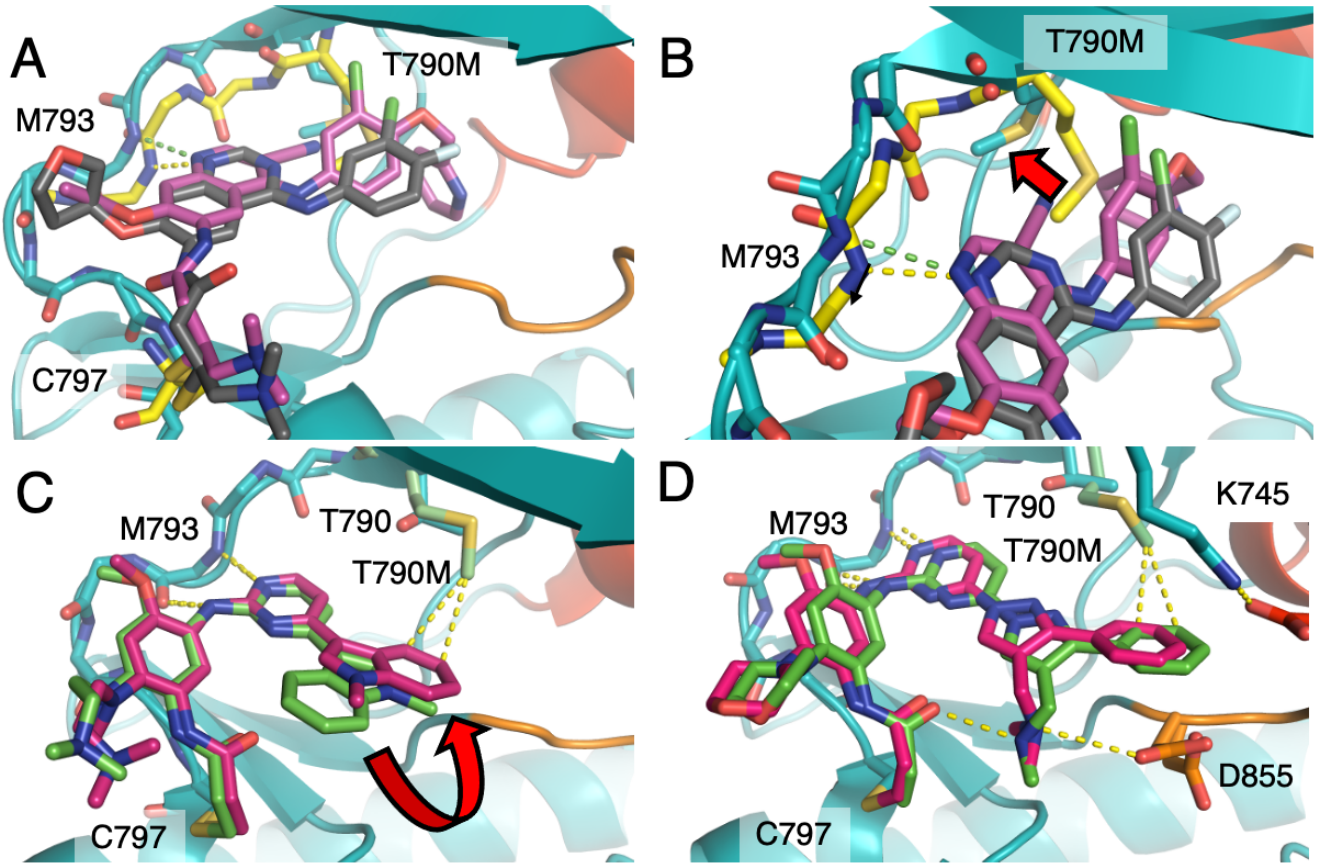

Figure 5. **Structural basis for potency differences with T790M.** Crystal structure overlays of (A) afatinib (grey/yellow, PDB ID 4G5P) and neratinib (magenta/teal, PDB ID 2JIV) with T790M EGFR. (B) Afatinib (grey/yellow, PDB ID 4G5P) and neratinib (magenta/teal, PDB ID 2JIV) with T790M magnified to highlight shift of T790M. Red arrow highlights the shift in position of the T790M side chain due to the steric effects from neratinib binding compared to afatinib. (C) osimertinib with WT EGFR (green, PDB ID 6JXT) and T790M EGFR (magenta, PDB ID 6JX0). Red arrow highlights the rotation of the *N*-methylindole for WT versus T790M mutant, which allows for the enhanced mutant selectivity seen in osimertinib. (D) lazertinib with WT EGFR (magenta, PDB ID 7UKV) and T790M EGFR (green, PDB ID 7UKW).

Potency trends related to binding modes.

Associating TKI activity in the context of available structural information is helpful to understand future development of improved pharmacological agents. With the trends in true and apparent potency seen in Figure 4, important inclinations can be seen regarding the impact of the T790M variant. Earlier work on anilinoquinazoline inhibitors, and our discussion above, shows that the first and second-generation TKIs all anchor phenyl rings in HRII directly across from the gatekeeper side chain. The phenyl ring in neratinib that extends into HRII requires closer binding of this ring near the gatekeeper, which is not the case for afatinib (Figure 5A and B). Accordingly, potency values against L858R/T790M are diminished for neratinib compared to afatinib indicating this steric clash with T790M is more

detrimental for type 1.5 neratinib.[37] On the other hand, T790M selectivity for osimertinib has been shown to be caused by unique van der Waals interactions with T790M, and made possible due to elaboration of hydrophobic groups inside the AdR (Figure 5C).[51] This interaction is enabled by the rotational flexibility of the *N*-methylindole of osimertinib, where this moiety is found rotated by ~180° in WT cocrystal structures and MD simulations.[51] The superior mutant selectivity of lazertinib (Table 1, Figure 4), when compared to osimertinib, can be attributed to similar van der Waals contacts with T790M (Figure 5C), but where a pendant amine in the AdR for lazertinib enables distinctive intramolecular H-bonding for rigidification of this inhibitor orientation (Figure 5D).[53] The fact that these structural differences correlate with differences in apparent potency values as determined using the 100x PCA method (Table 1) offer insights that guide design of novel modifications in the design of clinically important covalent compounds with selectivity for the mutant variants, while sparing the WT protein, to improve therapeutic efficacy.

Outlook and conclusions.

The rapid growth in popularity of small-molecule inhibitors that form covalent bonds, reversibly and irreversibly, is well-justified in drug discovery. Despite this positive trend, we find that potency measurements are generally difficult to compare from literature studies and this represents a challenge that requires diligence in reporting detailed compound treatment and assay conditions. This perspective highlights a variety of factors that influence data generation and offer considerations for ideal interpretation to make informed decisions in drug design.

For the characterization of a series of drug candidates and comparison to results published in the literature, it important to describe in detail and compare the compound treatment and assay conditions. In many cases, published reports may provide insufficient details that make accurate comparisons to any given study impractical. Different laboratories may also use alternative liquid handling and mixing protocols, that need to be considered. As presented in this perspective, inhibitor-specific properties such as TPSA can variably impact potency measurements and ensuring experimental protocols for maximal inhibitor solubility are necessary for parameter accuracy (10x vs 100x PCA). Additionally, for a variety of reasons, such as differing experimental methods or even confusing use of kinetic constants (K_i versus K_I), it is unlikely that results from previous studies will approximate each other (Table 1) and the most appropriate utility of the literature is based on the trends (e.g., rank order of potency) between inhibitors and enzyme target variants. Importantly, we emphasize that any potency assessments should include appropriate controls with the same conditions as the experimental inhibitors.

We and other groups have also found that the power of using a continuous assay format to generate potency values by complete progress curve analysis (PCA) with a global fit greatly improves ease of use, reproducibility, and the quality of the data generated as seen with the Sox-based PhosphoSens platform. This is especially true with the determination of k_{inact}/K_I values with covalent inhibitors. Additionally, we have shown that a plot of k_{inact}/K_I values normalized to WT is informative for assessing the selectivity of covalent inhibitors that target EGFR mutations and that this can be done effectively with both apparent and true potency values. While differences in true k_{inact}/K_I values supply the most rigorous differences in selectivity, apparent values may more accurately reflect time-dependent inhibition of EGFR variants that are dependent on K_M values for ATP and, where a comparison can be performed using the ATP K_M and 1 mM ATP, the latter can be used to more closely model biological conditions. It is expected that covalent inhibitors will continue to be discovered and developed across diverse targets and diseases, and the experimental considerations and data analysis reviewed here offer valuable perspectives and should inform decision making broadly in medicinal chemistry.

Table 1. The impact on liquid handling protocol on time-dependent inhibition behavior of AZD9291, YH25448, and LN2057.

Compound	Protocol	WT			L858R			L858R/T790M			Reference
		k_{inact} $\times 10^{-3}$ (s^{-1})	K_I^{app} (nM)	$(k_{inact}/K_I)^{app}$ $\times 10^5$ ($M^{-1}s^{-1}$)	k_{inact} $\times 10^{-3}$ (s^{-1})	K_I^{app} (nM)	$(k_{inact}/K_I)^{app}$ $\times 10^5$ ($M^{-1}s^{-1}$)	k_{inact} $\times 10^{-3}$ (s^{-1})	K_I^{app} (nM)	$(k_{inact}/K_I)^{app}$ $\times 10^5$ ($M^{-1}s^{-1}$)	
AZD9291 (osimertinib)	PCA 10x	11.5 ± 0.70	434 ± 32	0.264 ± 0.004	n.d.	n.d.	n.d.	10.8 ± 0.6	256 ± 16	0.424 ± 0.006	[53]
	PCA 100x	7.20 ± 0.46	34.4 ± 3.3	2.09 ± 0.10	6.36 ± 0.29	4.47 ± 0.3	14.2 ± 0.40	7.60 ± 0.61	16.4 ±1.7	4.63 ± 0.14	*This work*
	PCA	n.d	n.d.	0.011 ± 0.01	n.d.	n.d.	0.69 ± 0.02	n.d.	n.d.	0.49 ± 0.07	[50]
	SF[a]	36 ± 1	-	-	110 ± 20	-	-	120 ± 10	-	-	
	IC_{50}(t)	7.2 ± 1.8	14 ± 2.3	5.2 ± 0.5	5.0 ± 0.1	1.6± 0.3	32 ± 5	5.5 ± 1	1.5 ±0.1	38 ± 4	[59, 66, 67]
YH25448 (lazertinib)	PCA 10x	9.71 ± 0.45	271 ± 15	0.358 ± 0.04	n.d.	n.d.	n.d.	3.92 ± 0.07	34 ± 1.1	1.15 ± 0.02	[53]
	PCA 100x	6.51 ± 0.62	72.1 ± 8.5	0.903 ± 0.026	5.88 ± 0.34	4.68 ± 0.33	12.6 ± 0.3	5.20 ± 0.23	14.6 ± 0.8	3.56 ± 0.05	*This work*
LN2057	PCA 10x	5.59 ± 0.18	98.9 ± 3.9	0.565 ± 0.006	n.d.	n.d.	n.d.	9.35± 0.69	224 ± 19	0.418 ± 0.007	[53]
	PCA 100x	3.84 ± 0.18	11.4 ± 0.9	3.37 ± 0.013	7.17 ± 0.25	1.27 ± 0.06	56.6 ± 0.13	7.43 ± 0.33	32.5 ± 1.8	2.29 ± 0.4	*This work*
	IC_{50}(t)	2.7± 1	14±2.3	1.5 ± 0.4	0.5± 0.2	0.10± 0.03	1.3 ± 0.3	2.2± 0.05	0.10± 0.01	1.1 ± 0.2	[59, 66, 67]

n.d. = "not determined", PCA = "Progress curve analysis" (Sox-based substrate reagent), 10x = "10x 10% DMSO Inhibitor stock" liquid handling protocol, 100x = "100x 100% DMSO Inhibitor stock" liquid handling protocol, IC_{50}(t) = "incubation time-dependent potency", [a] all values aside from k_{inact} cannot be determined by stopped-flow double mixing. Enzyme concentrations and sources for "*This work"* rows = 4 nM EGFR WT GST-tagged, 4 nM EGFR [T790M/L858R], GST-tagged, Carna, 0.5 nM EGFR [L858R] GST-tagged, SignalChem**.**

Table 2. Recombinant enzyme source and buffer additives minimally impact time-dependent inhibition of EGFR WT and mutations with AZD9291.

Compound	Enzyme Supplier	Additives	WT			L858R			L858R/T790M		
			k_{inact} $\times 10^{-3}$ (s^{-1})	K_I^{app} (nM)	$(k_{inact}/K_I)^{app}$ $\times 10^5$ ($M^{-1}s^{-1}$)	k_{inact} $\times 10^{-3}$ (s^{-1})	K_I^{app} (nM)	$(k_{inact}/K_I)^{app}$ $\times 10^5$ ($M^{-1}s^{-1}$)	k_{inact} $\times 10^{-3}$ (s^{-1})	K_I^{app} (nM)	$(k_{inact}/K_I)^{app}$ $\times 10^5$ ($M^{-1}s^{-1}$)
AZD9291 (osimertinib)	SignalChem	TCEP/No BSA	6.52 ± 0.55	14.4 ± 1.6	4.54 ± 0.15	6.36 ± 0.29	4.47± 0.30	14.2 ± 0.4	7.98 ± 0.51	8.05 ± 0.66	9.92 ± 0.26
	Carna	TCEP/No BSA	7.2 ± 0.46	34.4 ± 3.30	2.09± 0.1	8.56± 0.5	6.51± 0.54	13.1 ± 0.4	7.60 ± 0.61	16.40 ± 1.70	4.63 ± 0.14
	SingalChem	DTT/BSA	n.d.	n.d.	n.d.	5.34 ± 0.22	3.91 ± 0.22	13.7 ± 0.34	n.d.	n.d.	n.d.
	Carna	DTT/BSA	3.14± 0.18	25.3 ± 2.4	1.24± 0.054	n.d.	n.d.	n.d.	4.77 ± 0.16	7.41 ± 0.36	6.44 ± 0.14

n.d. = "not determined", Enzyme concentrations and sources 4 nM EGFR WT, Carna; 0.5 nM EGFR [L858R], SignalChem; 4 nM EGFR [T790M/L858R], Carna; 0.5 nM EGFR WT SignalChem; 5.0 nM EGFR [T790M/L858R] SignalChem; 2.0 nM EGFR [L858R], Carna. Details about commercially available protein can be found in the SI.

Table 3. Time-dependent inhibition of EGFR enzymes with second-generation TKIs

Compound	Method	WT			L858R			L858R/T790M			Reference
		k_{inact} $\times 10^{-3}$ (s^{-1})	K_I^{app} (nM)	$(k_{inact}/K_I)^{app}$ $\times 10^5$ ($M^{-1}s^{-1}$)	k_{inact} $\times 10^{-3}$ (s^{-1})	K_I^{app} (nM)	$(k_{inact}/K_I)^{app}$ $\times 10^5$ ($M^{-1}s^{-1}$)	k_{inact} $\times 10^{-3}$ (s^{-1})	K_I^{app} (nM)	$(k_{inact}/K_I)^{app}$ $\times 10^5$ ($M^{-1}s^{-1}$)	
Afatinib	PCA 100x	4.44 ± 0.14	0.65 ± 0.03	68.7 ± 0.16	n.d.	n.d	298 ± 11	5.40 ± 0.17	45.3 ± 2.0	1.19 ± 0.02	*This work*
	PCA	n.d.	n.d.	2.0± 0.4	n.d.	n.d.	22±1	n.d.	n.d.	1.5 ± 0.2	[50]
	SF[a]	n.r.	-	-	n.r.	-	-	1.5±0.1	-	-	
	PCA	0.9± 0.1	n.r.	n.r.	n.r.	n.r.	n.r.	2.4± 0.3	n.r.	n.r.	[55]
Neratinib	PCA 100x	8.03 ± 0.78	6.88 ± 0.8	11.7 ± 0.3	6.34 ± 0.29	0.53 ± 0.03	118 ± 3	4.51 ± 0.19	121 ± 8	0.372 ± 0.11	*This work*
	PCA	1.8 ± 0.1	n.d.	n.d.	n.d.	n.d.	n.d.	1.1 ± 0.2	n.d.	n.d.	[55]
CI-1033 Canertinib	PCA 100x	5.57 ± 0.16	8.93 ± 0.72	40.4 ± 0.8	8.93 ± 0.72	0.05 ± 0.01	1700 ± 80	7.1 ± 0.35	5.27 ± 0.34	13.5 ± 0.3	*This work*
	PCA	2.9 ±1.9	n.r.	n.r.	n.r.	n.r.	n.r.	11.0±0.2	n.r.	n.r.	[55]

n.d. = "not determined", due to unambiguous two-step model due to inability to reach maximal inactivation rate (k_{inact}) at high afatinib concentration. n.r. indicates values that are not reported. [a] all values aside from k_{inact} cannot be determined by stopped-flow double mixing. Enzyme concentrations and sources for "*This work"* rows = 4 nM EGFR WT GST-tagged, 4 nM EGFR [T790M/L858R], GST-tagged, Carna, 0.5 nM EGFR [L858R] GST-tagged, SignalChem**.**

Acknowledgements

D.E.H. is supported by startup funds from the State University of New York and the National Center for Advancing Translational Sciences of the National Institutes of Health under award Number UL1TR001412-08 (BTC K Scholar Award to DEH). S.A.L. and iFIT are funded by the Deutsche Forschungsgemeinschaft (DFG, German Research Foundation) under Germany's Excellence Strategy (EXC 2180-390900677). TüCAD2 is funded by the Federal Ministry of Education and Research (BMBF) and the Baden-Württemberg Ministry of Science as part of the Excellence Strategy of the German Federal and State Governments.

Conflicts of Interest

D.U., E.S., and E.M. are employees and shareholders of AssayQuant Technologies, Inc., a provider of life science tool products and services that support drug discovery, including the PhosphoSens platform used to generate the data presented in this perspective.

Abbreviations

AdR, adenosine-binding region
BSA- bovine serum albumin
EGFR - epidermal growth factor receptor
WT- wild-type
TKI - tyrosine kinase inhibitor
HRI - hydrophobic region I
HRII - hydrophobic region II
TSPA - topological polar surface area
H-bond - hydrogen bond
K_i, dissociation constant
K_I, inactivation constant
K_M, Michaelis constant
k_{obs}, observed rate constant
SF, stopped flow
PCA, progress curve analysis
TCEP, tris(2-carboxyethyl)phosphine
DTT, dithiothreitol
app, apparent
SAR, structure activity relationship
SKR, structure kinetic relationship

References Cited

1. Singh, J., The Ascension of Targeted Covalent Inhibitors. *J. Med. Chem.* **2022,** *65* (8), 5886-5901.
2. Ghosh, A. K.; Samanta, I.; Mondal, A.; Liu, W. R., Covalent Inhibition in Drug Discovery. *ChemMedChem* **2019,** *14* (9), 889-906.
3. Boike, L.; Henning, N. J.; Nomura, D. K., Advances in covalent drug discovery. *Nature Reviews Drug Discovery* **2022,** *21* (12), 881-898.
4. Faridoon; Ng, R.; Zhang, G.; Li, J. J., An update on the discovery and development of reversible covalent inhibitors. *Medicinal Chemistry Research* **2023**, 1-24.
5. Schaefer, D.; Cheng, X., Recent Advances in Covalent Drug Discovery. *Pharmaceuticals* **2023,** *16* (5), 663.
6. Sutanto, F.; Konstantinidou, M.; Dömling, A., Covalent inhibitors: a rational approach to drug discovery. *RSC Medicinal Chemistry* **2020,** *11* (8), 876-884.
7. Copeland, R. A., The drug–target residence time model: a 10-year retrospective. *Nature Reviews Drug Discovery* **2016,** *15* (2), 87-95.
8. Han, W.; Du, Y., Recent Development of the Second and Third Generation Irreversible Epidermal Growth Factor Receptor Inhibitors. *Chemistry & Biodiversity* **2017,** *14* (7), e1600372.
9. Akinleye, A.; Chen, Y.; Mukhi, N.; Song, Y.; Liu, D., Ibrutinib and novel BTK inhibitors in clinical development. *Journal of hematology & oncology* **2013,** *6*, 1-9.
10. Gabizon, R.; London, N., A fast and clean BTK inhibitor. *J. Med. Chem.* **2020,** *63* (10), 5100-5101.
11. Ostrem, J. M.; Peters, U.; Sos, M. L.; Wells, J. A.; Shokat, K. M., K-Ras (G12C) inhibitors allosterically control GTP affinity and effector interactions. *Nature* **2013,** *503* (7477), 548-551.
12. Janes, M. R.; Zhang, J.; Li, L.-S.; Hansen, R.; Peters, U.; Guo, X.; Chen, Y.; Babbar, A.; Firdaus, S. J.; Darjania, L.; Feng, J.; Chen, J. H.; Li, S.; Li, S.; Long, Y. O.; Thach, C.; Liu, Y.; Zarieh, A.; Ely, T.; Kucharski, J. M.; Kessler, L. V.; Wu, T.; Yu, K.; Wang, Y.; Yao, Y.; Deng, X.; Zarrinkar, P. P.; Brehmer, D.; Dhanak, D.; Lorenzi, M. V.; Hu-Lowe, D.; Patricelli, M. P.; Ren, P.; Liu, Y., Targeting KRAS Mutant Cancers with a Covalent G12C-Specific Inhibitor. *Cell* **2018,** *172* (3), 578-589.e17.
13. Zhang, Z.; Morstein, J.; Ecker, A. K.; Guiley, K. Z.; Shokat, K. M., Chemoselective Covalent Modification of K-Ras(G12R) with a Small Molecule Electrophile. *J. Am. Chem. Soc.* **2022,** *144* (35), 15916-15921.
14. Zhang, Z.; Guiley, K. Z.; Shokat, K. M., Chemical acylation of an acquired serine suppresses oncogenic signaling of K-Ras(G12S). *Nature Chemical Biology* **2022,** *18* (11), 1177-1183.
15. Owen, D. R.; Allerton, C. M. N.; Anderson, A. S.; Aschenbrenner, L.; Avery, M.; Berritt, S.; Boras, B.; Cardin, R. D.; Carlo, A.; Coffman, K. J.; Dantonio, A.; Di, L.; Eng, H.; Ferre, R.; Gajiwala, K. S.; Gibson, S. A.; Greasley, S. E.; Hurst, B. L.; Kadar, E. P.; Kalgutkar, A. S.; Lee, J. C.; Lee, J.; Liu, W.; Mason, S. W.; Noell, S.; Novak, J. J.; Obach, R. S.; Ogilvie, K.; Patel, N. C.; Pettersson, M.; Rai, D. K.; Reese, M. R.; Sammons, M. F.; Sathish, J. G.; Singh, R. S. P.; Steppan, C. M.; Stewart, A. E.; Tuttle, J. B.; Updyke, L.; Verhoest, P. R.; Wei, L.; Yang, Q.; Zhu, Y., An oral SARS-CoV-2 M^{pro} inhibitor clinical candidate for the treatment of COVID-19. *Science* **2021,** *374* (6575), 1586-1593.
16. Gehringer, M.; Laufer, S. A., Emerging and Re-Emerging Warheads for Targeted Covalent Inhibitors: Applications in Medicinal Chemistry and Chemical Biology. *J. Med. Chem.* **2019,** *62* (12), 5673-5724.
17. Ray, S.; Murkin, A. S., New Electrophiles and Strategies for Mechanism-Based and Targeted Covalent Inhibitor Design. *Biochemistry* **2019,** *58* (52), 5234-5244.

18. de Bono, J. S.; Rowinsky, E. K., The ErbB receptor family: a therapeutic target for cancer. *Trends in molecular medicine* **2002,** *8* (4), S19-S26.
19. Hynes, N. E.; MacDonald, G., ErbB receptors and signaling pathways in cancer. *Current opinion in cell biology* **2009,** *21* (2), 177-184.
20. Eck, M. J.; Yun, C.-H., Structural and mechanistic underpinnings of the differential drug sensitivity of EGFR mutations in non-small cell lung cancer. *Biochimica et Biophysica Acta (BBA) - Proteins and Proteomics* **2010,** *1804* (3), 559-566.
21. Heppner, D. E.; Eck, M. J., A structural perspective on targeting the RTK/Ras/MAP kinase pathway in cancer. *Protein Sci.* **2021,** *30* (8), 1535-1553.
22. Paez, J. G.; Jänne, P. A.; Lee, J. C.; Tracy, S.; Greulich, H.; Gabriel, S.; Herman, P.; Kaye, F. J.; Lindeman, N.; Boggon, T. J., EGFR mutations in lung cancer: correlation with clinical response to gefitinib therapy. *Science* **2004,** *304* (5676), 1497-1500.
23. Lynch, T. J.; Bell, D. W.; Sordella, R.; Gurubhagavatula, S.; Okimoto, R. A.; Brannigan, B. W.; Harris, P. L.; Haserlat, S. M.; Supko, J. G.; Haluska, F. G., Activating mutations in the epidermal growth factor receptor underlying responsiveness of non–small-cell lung cancer to gefitinib. *N. Engl. J. Med.* **2004,** *350* (21), 2129-2139.
24. Soria, J.-C.; Ohe, Y.; Vansteenkiste, J.; Reungwetwattana, T.; Chewaskulyong, B.; Lee, K. H.; Dechaphunkul, A.; Imamura, F.; Nogami, N.; Kurata, T., Osimertinib in untreated EGFR-mutated advanced non–small-cell lung cancer. *N. Engl. J. Med.* **2018,** *378* (2), 113-125.
25. Zhou, W.; Ercan, D.; Chen, L.; Yun, C.-H.; Li, D.; Capelletti, M.; Cortot, A. B.; Chirieac, L.; Iacob, R. E.; Padera, R.; Engen, J. R.; Wong, K.-K.; Eck, M. J.; Gray, N. S.; Jänne, P. A., Novel mutant-selective EGFR kinase inhibitors against EGFR T790M. *Nature* **2009,** *462* (7276), 1070-1074.
26. Niederst, M. J.; Hu, H.; Mulvey, H. E.; Lockerman, E. L.; Garcia, A. R.; Piotrowska, Z.; Sequist, L. V.; Engelman, J. A., The allelic context of the C797S mutation acquired upon treatment with third-generation EGFR inhibitors impacts sensitivity to subsequent treatment strategies. *Clin. Cancer Res.* **2015,** *21* (17), 3924-3933.
27. Thress, K. S.; Paweletz, C. P.; Felip, E.; Cho, B. C.; Stetson, D.; Dougherty, B.; Lai, Z.; Markovets, A.; Vivancos, A.; Kuang, Y.; Ercan, D.; Matthews, S. E.; Cantarini, M.; Barrett, J. C.; Jänne, P. A.; Oxnard, G. R., Acquired EGFR C797S mutation mediates resistance to AZD9291 in non–small cell lung cancer harboring EGFR T790M. *Nat. Med.* **2015,** *21* (6), 560-562.
28. Damghani, T.; Wittlinger, F.; Beyett, T. S.; Eck, M. J.; Laufer, S. A.; Heppner, D. E., Chapter Six - Structural elements that enable specificity for mutant EGFR kinase domains with next-generation small-molecule inhibitors. In *Methods in Enzymology*, Richard, J. P.; Moran, G. R., Eds. Academic Press: 2023; Vol. 685, pp 171-198.
29. Zhao, H.-Y.; Xi, X.-X.; Xin, M.; Zhang, S.-Q., Overcoming C797S mutation: The challenges and prospects of the fourth-generation EGFR-TKIs. *Bioorg. Chem.* **2022,** *128*, 106057.
30. Ahn, M.-J.; Han, J.-Y.; Lee, K. H.; Kim, S.-W.; Kim, D.-W.; Lee, Y.-G.; Cho, E. K.; Kim, J.-H.; Lee, G.-W.; Lee, J.-S.; Min, Y. J.; Kim, J.-S.; Lee, S. S.; Kim, H. R.; Hong, M. H.; Ahn, J. S.; Sun, J.-M.; Kim, H. T.; Lee, D. H.; Kim, S.; Cho, B. C., Lazertinib in patients with EGFR mutation-positive advanced non-small-cell lung cancer: results from the dose escalation and dose expansion parts of a first-in-human, open-label, multicentre, phase 1–2 study. *Lancet Oncol.* **2019,** *20* (12), 1681-1690.
31. Yun, J.; Hong, M. H.; Kim, S.-Y.; Park, C.-W.; Kim, S.; Yun, M. R.; Kang, H. N.; Pyo, K.-H.; Lee, S. S.; Koh, J. S., YH25448, an irreversible EGFR-TKI with potent intracranial activity in EGFR mutant non–small cell lung cancer. *Clin. Cancer Res.* **2019,** *25* (8), 2575-2587.
32. Liu, Y.; Gray, N. S., Rational design of inhibitors that bind to inactive kinase conformations. *Nature Chemical Biology* **2006,** *2* (7), 358-364.

33. Solca, F.; Dahl, G.; Zoephel, A.; Bader, G.; Sanderson, M.; Klein, C.; Kraemer, O.; Himmelsbach, F.; Haaksma, E.; Adolf, G. R., Target Binding Properties and Cellular Activity of Afatinib (BIBW 2992), an Irreversible ErbB Family Blocker. *Journal of Pharmacology and Experimental Therapeutics* **2012,** *343* (2), 342-350.
34. Dungo, R. T.; Keating, G. M., Afatinib: first global approval. *Drugs* **2013,** *73* (13), 1503-1515.
35. Sun, H.; Wu, Y.-L., Dacomitinib in non-small-cell lung cancer: A comprehensive review for clinical application. *Future Oncol.* **2019,** *15* (23), 2769-2777.
36. Smaill, J. B.; Rewcastle, G. W.; Loo, J. A.; Greis, K. D.; Chan, O. H.; Reyner, E. L.; Lipka, E.; Showalter, H. D. H.; Vincent, P. W.; Elliott, W. L.; Denny, W. A., Tyrosine Kinase Inhibitors. 17. Irreversible Inhibitors of the Epidermal Growth Factor Receptor: 4-(Phenylamino)quinazoline- and 4-(Phenylamino)pyrido[3,2-d]pyrimidine-6-acrylamides Bearing Additional Solubilizing Functions. *J. Med. Chem.* **2000,** *43* (7), 1380-1397.
37. Bose, P.; Ozer, H., Neratinib: an oral, irreversible dual EGFR/HER2 inhibitor for breast and non-small cell lung cancer. *Expert opinion on investigational drugs* **2009,** *18* (11), 1735-1751.
38. Jia, Y.; Yun, C.-H.; Park, E.; Ercan, D.; Manuia, M.; Juarez, J.; Xu, C.; Rhee, K.; Chen, T.; Zhang, H.; Palakurthi, S.; Jang, J.; Lelais, G.; DiDonato, M.; Bursulaya, B.; Michellys, P.-Y.; Epple, R.; Marsilje, T. H.; McNeill, M.; Lu, W.; Harris, J.; Bender, S.; Wong, K.-K.; Jänne, P. A.; Eck, M. J., Overcoming EGFR(T790M) and EGFR(C797S) resistance with mutant-selective allosteric inhibitors. *Nature* **2016,** *534* (7605), 129-132.
39. De Clercq, D. J. H.; Heppner, D. E.; To, C.; Jang, J.; Park, E.; Yun, C.-H.; Mushajiang, M.; Shin, B. H.; Gero, T. W.; Scott, D. A.; Jänne, P. A.; Eck, M. J.; Gray, N. S., Discovery and Optimization of Dibenzodiazepinones as Allosteric Mutant-Selective EGFR Inhibitors. *ACS Med. Chem. Lett.* **2019,** *10* (11), 1549-1553.
40. To, C.; Jang, J.; Chen, T.; Park, E.; Mushajiang, M.; De Clercq, D. J.; Xu, M.; Wang, S.; Cameron, M. D.; Heppner, D. E., Single and dual targeting of mutant EGFR with an allosteric inhibitor. *Cancer Discov.* **2019,** *9* (7), 926-943.
41. Jang, J.; To, C.; De Clercq, D. J.; Park, E.; Ponthier, C. M.; Shin, B. H.; Mushajiang, M.; Nowak, R. P.; Fischer, E. S.; Eck, M. J.; Gray, Nathanael S., Mutant-Selective Allosteric EGFR Degraders are Effective Against a Broad Range of Drug-Resistant Mutations. *Angewandte Chemie International Edition* **2020,** *59* (34), 14481-14489.
42. Beyett, T. S.; To, C.; Heppner, D. E.; Rana, J. K.; Schmoker, A. M.; Jang, J.; De Clercq, D. J. H.; Gomez, G.; Scott, D. A.; Gray, N. S.; Jänne, P. A.; Eck, M. J., Molecular basis for cooperative binding and synergy of ATP-site and allosteric EGFR inhibitors. *Nat. Commun.* **2022,** *13* (1), 2530.
43. Gero, T. W.; Heppner, D. E.; Beyett, T. S.; To, C.; Azevedo, S. C.; Jang, J.; Bunnell, T.; Feru, F.; Li, Z.; Shin, B. H.; Soroko, K. M.; Gokhale, P. C.; Gray, N. S.; Jänne, P. A.; Eck, M. J.; Scott, D. A., Quinazolinones as allosteric fourth-generation EGFR inhibitors for the treatment of NSCLC. *Bioorganic Med. Chem. Lett.* **2022,** *68*, 128718.
44. Obst-Sander, U.; Ricci, A.; Kuhn, B.; Friess, T.; Koldewey, P.; Kuglstatter, A.; Hewings, D.; Goergler, A.; Steiner, S.; Rueher, D.; Imhoff, M.-P.; Raschetti, N.; Marty, H.-P.; Dietzig, A.; Rynn, C.; Ehler, A.; Burger, D.; Kornacker, M.; Schaffland, J. P.; Herting, F.; Pao, W.; Bischoff, J. R.; Martoglio, B.; Alice Nagel, Y.; Jaeschke, G., Discovery of Novel Allosteric EGFR L858R Inhibitors for the Treatment of Non-Small-Cell Lung Cancer as a Single Agent or in Combination with Osimertinib. *J. Med. Chem.* **2022,** *65* (19), 13052-13073.
45. To, C.; Beyett, T. S.; Jang, J.; Feng, W. W.; Bahcall, M.; Haikala, H. M.; Shin, B. H.; Heppner, D. E.; Rana, J. K.; Leeper, B. A.; Soroko, K. M.; Poitras, M. J.; Gokhale, P. C.; Kobayashi, Y.; Wahid, K.; Kurppa, K. J.; Gero, T. W.; Cameron, M. D.; Ogino, A.; Mushajiang, M.; Xu, C.; Zhang, Y.; Scott, D. A.; Eck, M. J.; Gray, N. S.; Jänne, P. A., An

allosteric inhibitor against the therapy-resistant mutant forms of EGFR in non-small cell lung cancer. *Nat. Cancer* **2022,** *3* (4), 402-417.
46. Li, Q.; Zhang, T.; Li, S.; Tong, L.; Li, J.; Su, Z.; Feng, F.; Sun, D.; Tong, Y.; Wang, X.; Zhao, Z.; Zhu, L.; Ding, J.; Li, H.; Xie, H.; Xu, Y., Discovery of Potent and Noncovalent Reversible EGFR Kinase Inhibitors of EGFRL858R/T790M/C797S. *ACS Med. Chem. Lett.* **2019,** *10* (6), 869-873.
47. Wittlinger, F.; Heppner, D. E.; To, C.; Günther, M.; Shin, B. H.; Rana, J. K.; Schmoker, A. M.; Beyett, T. S.; Berger, L. M.; Berger, B.-T.; Bauer, N.; Vasta, J. D.; Corona, C. R.; Robers, M. B.; Knapp, S.; Jänne, P. A.; Eck, M. J.; Laufer, S. A., Design of a "Two-in-One" Mutant-Selective Epidermal Growth Factor Receptor Inhibitor That Spans the Orthosteric and Allosteric Sites. *J. Med. Chem.* **2022,** *65* (2), 1370-1383.
48. Wittlinger, F.; Ogboo, B. C.; Pham, C. D.; Schaeffner, I. K.; Chitnis, S. P.; Damghani, T.; Beyett, T. S.; Rasch, A.; Buckley, B.; Urul, D. A.; Shaurova, T.; May, E. W.; Schaefer, E. M.; Eck, M. J.; Hershberger, P. A.; Laufer, S. A.; Heppner, D. E., Examining molecular factors of inactive versus active bivalent EGFR inhibitors: A missing link in fragment-based drug design. *ChemRxiv* **2023**, 10.26434/chemrxiv-2023-cs3xn.
49. Oxnard, G. R.; Thress, K. S.; Alden, R. S.; Lawrance, R.; Paweletz, C. P.; Cantarini, M.; Yang, J. C.-H.; Barrett, J. C.; Jänne, P. A., Association between plasma genotyping and outcomes of treatment with osimertinib (AZD9291) in advanced non–small-cell lung cancer. *Journal of clinical oncology* **2016,** *34* (28), 3375.
50. Zhai, X.; Ward, R. A.; Doig, P.; Argyrou, A., Insight into the Therapeutic Selectivity of the Irreversible EGFR Tyrosine Kinase Inhibitor Osimertinib through Enzyme Kinetic Studies. *Biochemistry* **2020,** *59* (14), 1428-1441.
51. Yan, X.-E.; Ayaz, P.; Zhu, S.-J.; Zhao, P.; Liang, L.; Zhang, C. H.; Wu, Y.-C.; Li, J.-L.; Choi, H. G.; Huang, X.; Shan, Y.; Shaw, D. E.; Yun, C.-H., Structural Basis of AZD9291 Selectivity for EGFR T790M. *J. Med. Chem.* **2020,** *63* (15), 8502-8511.
52. Shu, C. A.; Goto, K.; Ohe, Y.; Besse, B.; Lee, S.-H.; Wang, Y.; Griesinger, F.; Yang, J. C.-H.; Felip, E.; Sanborn, R. E.; Caro, R. B.; Curtin, J. C.; Chen, J.; Mahoney, J. M.; Trani, L.; Bauml, J. M.; Knoblauch, R. E.; Thayu, M.; Cho, B. C., Amivantamab and lazertinib in patients with EGFR-mutant non–small cell lung (NSCLC) after progression on osimertinib and platinum-based chemotherapy: Updated results from CHRYSALIS-2. *Journal of Clinical Oncology* **2022,** *40* (16_suppl), 9006-9006.
53. Heppner, D. E.; Wittlinger, F.; Beyett, T. S.; Shaurova, T.; Urul, D. A.; Buckley, B.; Pham, C. D.; Schaeffner, I. K.; Yang, B.; Ogboo, B. C.; May, E. W.; Schaefer, E. M.; Eck, M. J.; Laufer, S. A.; Hershberger, P. A., Structural Basis for Inhibition of Mutant EGFR with Lazertinib (YH25448). *ACS Med. Chem. Lett.* **2022,** *13* (12), 1856-1863.
54. Copeland, R. A., *Evaluation of enzyme inhibitors in drug discovery: a guide for medicinal chemists and pharmacologists*. John Wiley & Sons: 2013.
55. Schwartz, P. A.; Kuzmic, P.; Solowiej, J.; Bergqvist, S.; Bolanos, B.; Almaden, C.; Nagata, A.; Ryan, K.; Feng, J.; Dalvie, D.; Kath, J. C.; Xu, M.; Wani, R.; Murray, B. W., Covalent EGFR inhibitor analysis reveals importance of reversible interactions to potency and mechanisms of drug resistance. *Proc. Natl. Acad. Sci. U.S.A.* **2014,** *111* (1), 173-178.
56. Luković, E.; González-Vera, J. A.; Imperiali, B., Recognition-Domain Focused Chemosensors: Versatile and Efficient Reporters of Protein Kinase Activity. *J. Am. Chem. Soc.* **2008,** *130* (38), 12821-12827.
57. Shults, M. D.; Carrico-Moniz, D.; Imperiali, B., Optimal Sox-based fluorescent chemosensor design for serine/threonine protein kinases. *Analytical biochemistry* **2006,** *352* (2), 198-207.

58. Shults, M. D.; Janes, K. A.; Lauffenburger, D. A.; Imperiali, B., A multiplexed homogeneous fluorescence-based assay for protein kinase activity in cell lysates. *Nature methods* **2005,** *2* (4), 277-284.
59. Krippendorff, B.-F.; Neuhaus, R.; Lienau, P.; Reichel, A.; Huisinga, W., Mechanism-based inhibition: deriving KI and kinact directly from time-dependent IC50 values. *SLAS Discovery* **2009,** *14* (8), 913-923.
60. Kuzmič, P., A two-point IC₅₀ method for evaluating the biochemical potency of irreversible enzyme inhibitors. *bioRxiv* **2022**, 2020.06.25.171207.
61. Jia, Y., Current status of HTRF® technology in kinase assays. *Expert opinion on drug discovery* **2008,** *3* (12), 1461-1474.
62. Mons, E.; Roet, S.; Kim, R. Q.; Mulder, M. P. C., A Comprehensive Guide for Assessing Covalent Inhibition in Enzymatic Assays Illustrated with Kinetic Simulations. *Current Protocols* **2022,** *2* (6), e419.
63. Prasanna, S.; Doerksen, R., Topological polar surface area: a useful descriptor in 2D-QSAR. *Current medicinal chemistry* **2009,** *16* (1), 21-41.
64. Guha, R.; Dexheimer, T. S.; Kestranek, A. N.; Jadhav, A.; Chervenak, A. M.; Ford, M. G.; Simeonov, A.; Roth, G. P.; Thomas, C. J., Exploratory analysis of kinetic solubility measurements of a small molecule library. *Bioorganic Med. Chem. Lett.* **2011,** *19* (13), 4127-4134.
65. Karami, T. K.; Hailu, S.; Feng, S.; Graham, R.; Gukasyan, H. J., Eyes on Lipinski's Rule of Five: A New “Rule of Thumb” for Physicochemical Design Space of Ophthalmic Drugs. *Journal of Ocular Pharmacology and Therapeutics* **2022,** *38* (1), 43-55.
66. Engel, J.; Becker, C.; Lategahn, J.; Keul, M.; Ketzer, J.; Mühlenberg, T.; Kollipara, L.; Schultz-Fademrecht, C.; Zahedi, R. P.; Bauer, S.; Rauh, D., Insight into the Inhibition of Drug-Resistant Mutants of the Receptor Tyrosine Kinase EGFR. *Angewandte Chemie International Edition* **2016,** *55* (36), 10909-10912.
67. Günther, M.; Lategahn, J.; Juchum, M.; Döring, E.; Keul, M.; Engel, J.; Tumbrink, H. L.; Rauh, D.; Laufer, S., Trisubstituted pyridinylimidazoles as potent inhibitors of the clinically resistant L858R/T790M/C797S EGFR mutant: targeting of both hydrophobic regions and the phosphate binding site. *J. Med. Chem.* **2017,** *60* (13), 5613-5637.
68. Yun, C.-H.; Boggon, T. J.; Li, Y.; Woo, M. S.; Greulich, H.; Meyerson, M.; Eck, M. J., Structures of Lung Cancer-Derived EGFR Mutants and Inhibitor Complexes: Mechanism of Activation and Insights into Differential Inhibitor Sensitivity. *Cancer Cell* **2007,** *11* (3), 217-227.
69. Carey, K. D.; Garton, A. J.; Romero, M. S.; Kahler, J.; Thomson, S.; Ross, S.; Park, F.; Haley, J. D.; Gibson, N.; Sliwkowski, M. X., Kinetic analysis of epidermal growth factor receptor somatic mutant proteins shows increased sensitivity to the epidermal growth factor receptor tyrosine kinase inhibitor, erlotinib. *Cancer Res.* **2006,** *66* (16), 8163-8171.
70. Yun, C.-H.; Mengwasser, K. E.; Toms, A. V.; Woo, M. S.; Greulich, H.; Wong, K.-K.; Meyerson, M.; Eck, M. J., The T790M mutation in EGFR kinase causes drug resistance by increasing the affinity for ATP. *Proc. Natl. Acad. Sci. U.S.A.* **2008,** *105* (6), 2070-2075.
71. Yung-Chi, C.; Prusoff, W. H., Relationship between the inhibition constant (KI) and the concentration of inhibitor which causes 50 per cent inhibition (IC50) of an enzymatic reaction. *Biochemical pharmacology* **1973,** *22* (23), 3099-3108.
72. Burlingham, B. T.; Widlanski, T. S., An Intuitive Look at the Relationship of Ki and IC50: A More General Use for the Dixon Plot. *Journal of Chemical Education* **2003,** *80* (2), 214.